Princeton Plasma Physics Laboratory

PPPL- 5060

PPPL-5060

Statistical Simulation of the Magnetorotational Dynamo

J. Squire, and A. Bhattacharjee

AUGUST 2014

Prepared for the U.S. Department of Energy under Contract DE-AC02-09CH11466.

Princeton Plasma Physics Laboratory
Report Disclaimers

Full Legal Disclaimer

Trademark Disclaimer

PPPL Report Availability

Princeton Plasma Physics Laboratory:

http://www.pppl.gov/techreports.cfm

Office of Scientific and Technical Information (OSTI):

http://www.osti.gov/scitech/

Related Links:

U.S. Department of Energy

Office of Scientific and Technical Information

Statistical simulation of the magnetorotational dynamo

J. Squire[1] and A. Bhattacharjee[1,2]

[1]*Department of Astrophysical Sciences and Princeton Plasma Physics Laboratory, Princeton University, Princeton, NJ 08543*

[2]*Max Planck/Princeton Center for Plasma Physics, Princeton University, Princeton, NJ 08543*

Abstract

We analyze turbulence and dynamo induced by the magnetorotational instability (MRI) using quasi-linear statistical simulation methods. We find that homogenous turbulence is unstable to a large scale dynamo instability, which saturates to an inhomogenous equilibrium with a very strong dependence on the magnetic Prandtl number (Pm). Despite its enormously reduced nonlinearity, the quasi-linear model exhibits the same qualitative scaling of angular momentum transport with Pm as fully nonlinear turbulence. This demonstrates the relationship of recent convergence problems to the large scale dynamo and suggests possible methods for studying astrophysically relevant regimes at very low or high Pm.

PACS numbers: 52.30.Cv,47.20.Ft,97.10.Gz

Understanding the complex web of nonlinear interactions that are important for the sustenance of turbulence induced by the magnetorotational instability (MRI) [1] has proven to be a difficult undertaking. Indeed, despite many theoretical and computational studies, results with quantitative application to most regimes relevant for astrophysical disks remain elusive. The fundamental problem is that astrophysical objects generally contain an enormous range of dynamically important scales, as measured by the fluid and magnetic Reynolds numbers (Re and Rm respectively). Of course, any simulation is necessarily limited in its resolvable scales, and the question of whether a set of results would change significantly with resolution becomes subtle and very difficult to answer conclusively. In the case of MRI turbulence, all indications are that at currently available resolutions, simulation convergence depends on the details of the computational domain [2–8], and the scaling of pertinent quantities such as the turbulent momentum transport remains unclear. Of particular importance [9–12] is the scaling with magnetic Prandtl number Pm = Rm/Re; astrophysical objects invariably have very high or low Pm but these regimes are extremely computationally challenging. Indeed, it is currently unclear whether MRI turbulence is sufficiently virulent to explain observations in the very low Pm limit, since turbulent activity seems to decrease with Pm or disappear altogether [6, 9, 13] (but see [14]). A large-scale dynamo generating strong azimuthal magnetic fields [7, 15–17] seems to be a key component of the turbulence, although the exact nature of the interactions and importance of different effects (*e.g.,* vertical stratification, compressibility) remains unclear.

In this letter we study MRI turbulence and dynamo in the zero net-flux unstratified shearing box using novel quasi-linear statistical simulation methods [18, 19]. This involves driving an ensemble of linear fluctuations in mean fields that depend only on the vertical co-ordinate (z), with the nonlinear stresses of these fluctuations self-consistently driving evolution of the mean fields. Our motivation for this is two-fold: Firstly, despite being a rather recent subject, direct statistical simulation – the method of simulating flow *statistics* rather than an individual realization – has proven to be a useful computational technique in a variety of applications [20–23]. An equilibrium of the system is in general a *turbulent* state, and analysis of its stability properties and bifurcations can be very rewarding. Secondly, fully developed MRI turbulence is incredibly complex and we feel there is much useful insight to be gained by selectively *removing* important physical effects in the hope of discovering simple underlying principles. Motivated by the idea that strong linear MRI growth is possible at all scales due to nonmodal effects [24], our quasi-linear approximation involves neglecting almost all of the nonlinear interactions in the system (there is no nonlinear

cascade), and can easily be systematically reduced further.

Remarkably, despite the strongly reduced nonlinearity, we demonstrate that the qualitative dependence on Pm in the quasi-linear system is the same as fully nonlinear MRI turbulence. In particular, at fixed magnetic Reynolds number (Rm), an increase in Pm causes an increase in the intensity of the turbulence (as measured by the angular momentum transport), despite the fact that the system is becoming more dissipative. This illustrates that the strong Pm dependence of the MRI [9] is (at least partially) due to increased large-scale dynamo action at higher Pm, since this is the only physical effect retained in the quasi-linear model beyond simple excitation of linear waves (which show the opposite trend). As discussed, the statistical simulation method (from hereon we shall use the term second-order cumulant expansion (CE2) [19], although the term stochastic structural stability theory (S3T) [18] is also common and pertains to similar ideas) is very well suited to the study of bifurcations between turbulent states of the system. We see two important bifurcations – the first marking the onset of a dynamo instability of homogenous turbulence, the second a transition to a time-dependent state – and the Pm dependence of several aspects of these transitions is strongly suggestive. It is our hope that studying these may provide a viable path forward in understanding the most astrophysically relevant high and low Pm regimes. Note that the approach is quite distinct from, and complementary to, previous nonlinear dynamics work on MRI dynamo [25, 26], which has focused on searching for cycles and bifurcations in the full nonlinear system at low Reynolds numbers. Strong similarities can be drawn between the self-sustaining mechanisms suggested in these works and magnetic field generation in our CE2 model [20].

The starting point of our study is the local incompressible MHD equations in a shearing background in the rotating frame,

$$\begin{aligned}
&\frac{\partial \boldsymbol{u}}{\partial t} - q\Omega x\frac{\partial \boldsymbol{u}}{\partial y} + (\boldsymbol{u}\cdot\nabla)\,\boldsymbol{u} + 2\Omega\hat{\boldsymbol{z}}\times\boldsymbol{u} = \\
&\qquad -\nabla p + \boldsymbol{B}\cdot\nabla\boldsymbol{B} + q\Omega u_x\hat{\boldsymbol{y}} + \bar{\nu}\nabla^2\boldsymbol{u}, \\
&\frac{\partial \boldsymbol{B}}{\partial t} - q\Omega x\frac{\partial \boldsymbol{B}}{\partial y} = -q\Omega B_x\hat{\boldsymbol{y}} + \nabla\times(\boldsymbol{u}\times\boldsymbol{B}) + \bar{\eta}\nabla^2\boldsymbol{B}, \\
&\qquad \nabla\cdot\boldsymbol{u} = 0, \quad \nabla\cdot\boldsymbol{B} = 0.
\end{aligned} \tag{1}$$

These are obtained from the standard MHD equations for a disk with radial stratification by considering a small Cartesian volume (at r_0) co-rotating with the fluid at angular velocity $\Omega(r) \sim \Omega_0 r^{-q}$.

In this limit the velocity shear is linear, $\boldsymbol{U}_0 = -q\Omega x\hat{\boldsymbol{y}}$, and $\boldsymbol{u}$ denotes velocity fluctuations about this background. The directions x, y, z in Eq. (1) correspond respectively to the radial, azimuthal and vertical directions in the disk. The use of dimensionless variables in Eq. (1) means $\Omega \equiv \Omega(r_0) = 1$, and the bulk flow Reynolds numbers are $\mathrm{Re} = q/\bar{\nu}$, $\mathrm{Rm} = q/\bar{\eta}$. Throughout this work we consider a homogenous background (no stratification), with zero net magnetic flux, and use shearing box boundary conditions (periodic in y, z, periodic in the shearing frame in x) with an aspect ratio $\left(L_x, L_y, L_z\right) = (1, \pi, 1)$.

The basis of our application of CE2 to MRI turbulence is a splitting of Eq. (1) into its mean and fluctuating parts, as defined by the horizontal average, $\overline{f(\boldsymbol{x})}(z) \equiv (L_x L_y)^{-1} \int dxdy\, f(\boldsymbol{x})$. The motivation for this averaging is that it is the simplest possible that allows for the strong z-dependent B_y observed in nonlinear simulations [14, 15]. Schematically representing the state of the system $(\boldsymbol{u}, \boldsymbol{B}, P)$ as U, a decomposition of Eq. (1) into equations for $\bar{U}$ and $u' = U - \bar{U}$ leads to

$$\partial_t \bar{U} = \mathcal{A}_{mean} \cdot \bar{U} + \overline{\mathcal{R}(u', u')}, \tag{2a}$$

$$\partial_t u' = \mathcal{A}_{fluct}\left(\bar{U}\right) \cdot u' + \left\{\mathcal{R}(u', u') - \overline{\mathcal{R}(u', u')}\right\} + \xi_t \tag{2b}$$

where $\mathcal{A}_{mean}$ and $\mathcal{A}_{fluct}\left(\bar{U}\right)$ are the linear operators for the mean and fluctuating parts, $\mathcal{R}(u', u')$ represents the nonlinear stresses, and ξ_t is an additional white-in-time driving noise term. The principle approximation, which is key to CE2 and leads to the *quasi-linear* system, is to neglect the eddy-eddy nonlinearity $\left\{\mathcal{R}(u', u') - \overline{\mathcal{R}(u', u')}\right\}$ in Eq. (2b), meaning the only nonlinearity arises from the coupling to Eq. (2a). The driving noise ξ_t can be considered either a physical source of noise [19], or a particularly simple closure representing the effects of the neglected nonlinearity [18].

Rather than evolving the non-deterministic Eq. (2b), consider the single time correlation matrix of an ensemble of fluctuations $C_{ij}(\boldsymbol{x}_1, \boldsymbol{x}_2, t) = \left\langle u_i'(\boldsymbol{x}_1, t)\, u_j'(\boldsymbol{x}_2, t)\right\rangle$, where $\langle\cdot\rangle$ denotes the ensemble average over realizations of ξ_t. Multiplication of Eq. (2b) by $\partial_t u(\boldsymbol{x}_2)$ followed by an ensemble average leads to [18, 22]

$$\partial_t C = \mathcal{A}_{fluct}\left(\bar{U}\right) \cdot C + C \cdot \mathcal{A}_{fluct}\left(\bar{U}\right)^{\dagger} + Q, \tag{3}$$

where $Q = \langle \xi(\boldsymbol{x}_1, t)\, \xi(\boldsymbol{x}_2, t)\rangle$ is the spatial correlation of the noise [27]. Using homogeneity in x, y, Eq. (3) can be reduced to 4 dimensions with the change of variables, $x = x_1 - x_2$, $y = y_1 - y_2$.

Assuming ergodicity – the equivalence of the x, y and ensemble averages – the nonlinear stresses $\overline{\mathcal{R}(u', u')}$ in the mean field equations [Eq. (2a)] can be calculated directly from C. With this change Eqs. (2a) and (3) comprise the CE2 system. Aside from the driving noise, conservation laws are inherited from the full nonlinear system (*e.g.,* energy and magnetic helicity).

The MRI mean field equations are very simple,

$$\begin{aligned} \partial_t \left(\bar{U}_x, \bar{U}_y\right) &= \left(2\bar{U}_y, (q-2)\,\bar{U}_x\right) + \left(\mathcal{R}_x, \mathcal{R}_y\right) \\ \partial_t \left(\bar{B}_x, \bar{B}_y\right) &= \left(0, -q\bar{B}_x\right) + \left(\mathcal{M}_x, \mathcal{M}_y\right), \end{aligned} \tag{4}$$

with $\partial_z \bar{U}_z = \partial_z \bar{B}_z = 0$ due to the divergence constraints. The nonlinear stresses arising from the fluctuating variables, $\mathcal{R}_j = \overline{\left\langle -\left(\boldsymbol{u}' \cdot \nabla \boldsymbol{u}'\right)_j + \left(\boldsymbol{b}' \cdot \nabla \boldsymbol{b}'\right)_j \right\rangle}$ and $\mathcal{M}_j = \overline{\left\langle \left(\nabla \times \left(\boldsymbol{u}' \times \boldsymbol{b}'\right)\right)_j \right\rangle}$, are calculated by applying appropriate derivative operators to the C matrix. We solve for C in the variables, $u \equiv u'_x$, $b \equiv b'_x$, $\zeta \equiv \partial_z u'_y - \partial_y u'_z$, $\eta \equiv \partial_z b'_y - \partial_y b'_z$, which conveniently reduce the dimension of C and remove divergence constraints. The equations, however, become very complex and we do not reproduce them here (*Mathematica* scripts are used to automatically generate the required c++ code). We use a Fourier pseudo-spectral method (with 3/2 dealiasing) in the shearing frame with the remapping method of Ref. [28], and a semi-implicit Runge-Kutta time-integrator. Note that a CE2 system of m fluctuating fields requires a C grid of size $N_x \times N_y \times (mN_z)^2$, but a single run contains more information than the equivalent direct quasi-linear simulation.

In all calculations presented here, we initialize with $C = 0$. The spatial correlation of ξ_t is chosen to drive each mode equally in energy [20], multiplied by an amplitude factor f_ξ. While we have explored the dependence on f_ξ, for simplicity all calculations in this letter use the same value ($f_\xi = 4$ in our normalization) and we change the physical parameters Rm and Pm to illustrate bifurcations of the system. For reference, this noise level drives homogenous turbulence at Rm = 12000, Pm = 1 to a mean total energy of ~ 0.05. We have used resolutions up to $64\times128\times(4\times96)^2$ (note that dealiasing is not required in x and y), and tested conservation of energy to ensure grid dissipation is a minor effect.

The MRI dynamo instability In contrast to the original MRI equations [Eq. (1)], a general stable equilibrium of the CE2 system [Eqs. (3) and (4)] corresponds to a statistically stationary turbulent state within the quasi-linear approximation. If such an equilibrium is rendered unstable by a change in system parameters, this turbulent state is no longer possible and a rearrangement of the mean fields and flow statistics will occur. This type of instability has no counterpart in

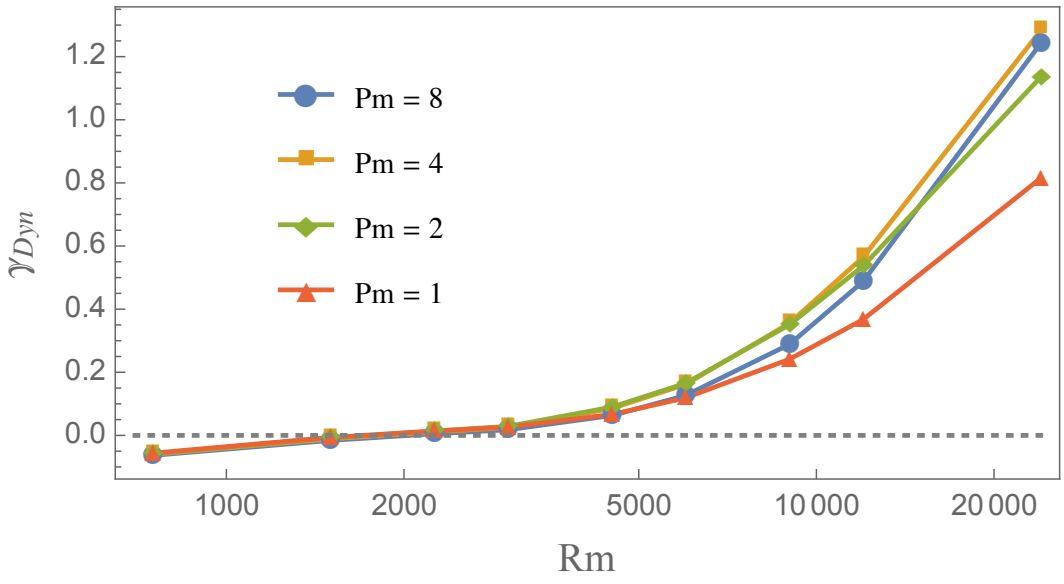

FIG. 1. Growth rate γ_{Dyn} of the mean field, $\bar{B}_y = \bar{B}_{y0}(z)\, e^{\gamma_{Dyn} t}$, as a function of magnetic Reynolds number at Pm = 1, 2, 4 and 8.

standard MHD stability theory; it pertains to the idea that the collective effect of the ensemble of fluctuating fields is to re-enforce perturbations to the mean fields through the nonlinear stresses, causing instability. Of course, such ideas are familiar in mean-field electrodynamics, and the CE2 method seems very well suited for more general study of large scale dynamos.

Homogenous turbulence, with $\left(\bar{\boldsymbol{U}}, \bar{\boldsymbol{B}}\right) = 0$, is the simplest non-trivial equilibrium of the CE2 MRI system, with all nonlinear stresses vanishing identically. However, at fixed noise, as the Reynolds numbers are increased from zero this equilibrium becomes unstable around Rm ≈ 1500 (note that noise can also be used as the bifurcation parameter). Such behavior is illustrated in Fig. 1, which shows the growth rate γ_{Dyn} of this dynamo instability. This is calculated by first evolving Eq. 3 to the homogenous equilibrium by artificially removing the nonlinear feedback, then introducing a very small ($\sim 10^{-15}$) random mean field (with the amplitudes of $\bar{\boldsymbol{U}}$, $\bar{B}_x$ 1/10 that of $\bar{B}_y$). (Note that it is quite possible to solve for the Floquet eigenspectrum of the system directly, although this is computationally challenging due to the grid size.) Following the introduction of mean-field feedback there is a sustained period of exponential growth in $\bar{\boldsymbol{B}}$ for Rm $\gtrsim 1500$. The observed eigenmodes are sinusoidal in z (as ensured by the spatial homogeneity) although not generally the largest mode in the box, satisfy $B_x \ll B_y$ and seem to have $\bar{\boldsymbol{U}} = 0$ [29]. While it is certainly expected that γ_{Dyn} increase strongly with Rm – fluctuations will grow to a higher amplitude and there is less $\bar{\boldsymbol{B}}$ dissipation – its dependence on Pm is more interesting and suggestive. An

increase in Pm implies an increase in dissipation (through increasing viscosity), yet Fig. 1 shows that γ_{Dyn} can increase, particularly at higher Rm. In addition, $\frac{\partial}{\partial \mathrm{Rm}}\gamma_{Dyn}\,(\mathrm{Rm})$ increases with Pm, with potentially interesting consequences for the very high Rm limit. The instability is driven by the radial stress $\mathcal{M}_x$ causing an increase in $\bar{B}_x$, which in turn drives $\bar{B}_y$ through the Ω effect, $-q\bar{B}_y$ [see Eq. (4)]. The effect of the azimuthal stress $\mathcal{M}_y$ is always negative. This is exactly the dynamo mechanism studied in detail in Refs. [15, 30], and has strong similarities to exact nonlinear dynamo solutions at low Rm [25, 26].

Of more relevance to fully developed turbulence are the saturation characteristics of the dynamo instability. To save computation, we initialize with moderately strong random mean fields (amplitude of $\bar{B}_y \approx 0.01$, $\bar{B}_x$ and $\bar{\boldsymbol{U}}$ initialized at 1/10 that of $\bar{B}_y$ – we have also studied initialization with the largest mode of the box obtaining similar results). As Rm is increased and homogenous equilibrium rendered unstable, the system saturates to a new CE2 equilibrium with a strong background $\bar{B}_y$ that varies on the largest scale in the box, as illustrated by the example in Fig. 2(a). As we increase Rm further, a second bifurcation occurs, at which the inhomogenous equilibrium appears to become unstable and the system transitions to a quasi-periodic time-dependent state. An example of this state, which occurs more readily at higher Pm, is shown in Fig. 2(b). These two bifurcations – first to an inhomogenous state dominated by mean fields, then the loss of equilibrium of this state – bear a strong resemblance to the transitions seen in hydrodynamic plane Couette flow [20], in which the second transition is associated with self-sustaining behavior. Such a self-sustaining process is not possible within our model due to our use of a single direction of inhomogeneity (as opposed to two in Ref. [20]), but the similarity as well as its Pm dependence is striking, and understanding physical mechanisms behind the loss of equilibrium may give useful insights into the self-sustaining dynamo that is so fundamental to zero net-flux turbulence.

This information is presented more compactly in Fig. 2(c), which illustrates the saturated $\bar{B}_y$ amplitude over a range of Rm, Pm. The dependence of the saturated amplitude on Pm is enormous (contrary to previous results on the large scale dynamo [31]), and can be well understood at low Rm using the linear properties of inhomogenous shearing waves [15, 30]. Interestingly, there is a marked *decrease* in the saturated amplitudes at all Pm as Rm is increased. We have been unable to find a convincing physical mechanism to explain this effect, but note that it depends critically on the interaction of the fluctuating fields with $\bar{B}_x$. This illustrates that some important physical effects may be absent from the saturation mechanism proposed in Refs. [15, 30]. Finally, we note that close to the critical point ($\mathrm{Rm} \approx 1500$) the supercritical nature of the bifurcation is evident,

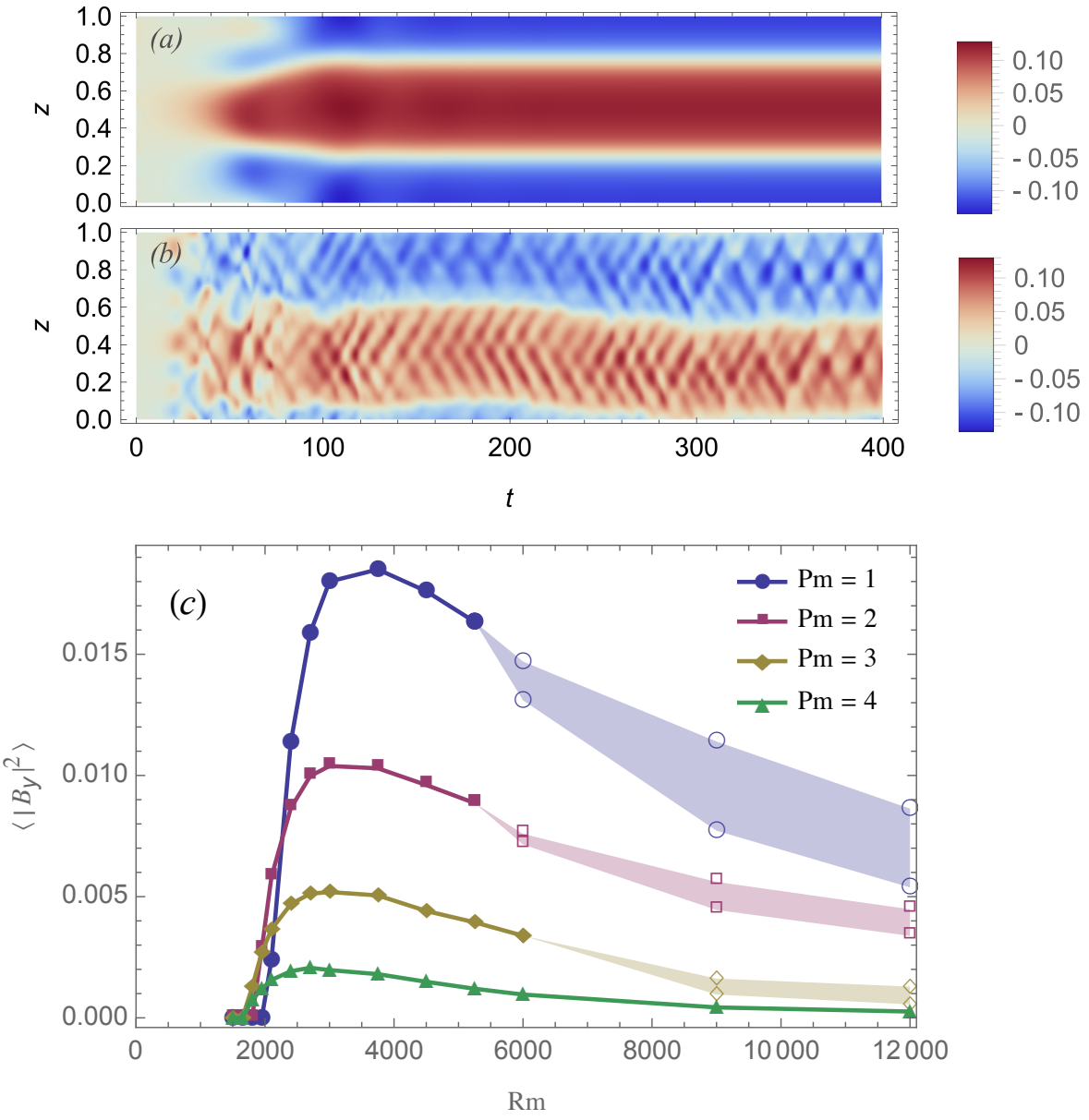

FIG. 2. Evolution of $\bar{B}_y$ as a function of (z, t) at Pm = 4 for (a) Rm = 4500, time-independent saturated state, and (b) Rm = 12000, time-dependent saturated state. (c) Magnitude of $\bar{B}_y$ as measured by $\frac{1}{L_z}\int dz \left|\bar{B}_y\right|^2$ at saturation, as a function of Rm for Pm = 1 → 8. The shaded regions illustrate the approximate maxima and minima of the time-dependent $\bar{B}_y$ when the system did not reach a time-independent statistical equilibrium (the exact values given here are necessarily a little subjective, particularly for Pm = 2, which exhibits much lower frequency oscillations of a somewhat different character).

and the process should be well described by a real Ginzburg-Landau equation about this point [23].

In Fig. 3 we present the angular momentum transport as a function of time for the highest Rm calculations presented in Fig. 2. The increase in transport with Pm despite the increased dissipation

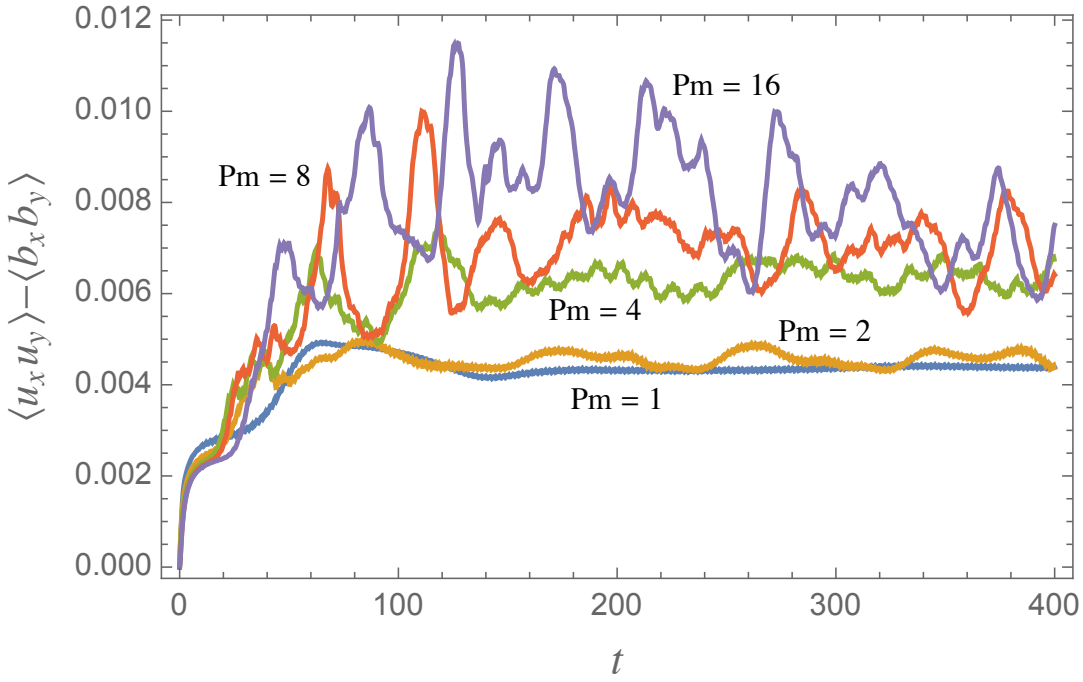

FIG. 3. Angular momentum transport $\left\langle u_x u_y \right\rangle - \left\langle b_x b_y \right\rangle$ (including mean and fluctuating variables) as a function of time for Rm = 12000, Pm = 1 → 16.

is evident, suggesting a direct relationship between shearing box convergence problems [9, 10] and the large scale dynamo. While the scaling is not so pronounced as self-sustained non-linear turbulence (see *e.g.,* Ref. [9] figure 7), this is to be expected since the CE2 calculations are driven: even without nonlinearity there is a base level of transport due to linear wave excitation (which shows the opposite trend with Pm). Future work will study this scaling in more quantitative detail [32] through comparison with driven nonlinear simulation. Note that the increase in transport is not primarily from the contribution of the mean fields directly (*e.g.,* through $\left\langle \bar{B}_x \bar{B}_y \right\rangle$), but rather due to the fluctuations becoming more intense as a consequence of the stronger mean fields.

Discussion Our primary motivation for this work has been to disentangle the important processes involved in MRI turbulence and dynamo. With this aim, we have enormously reduced the nonlinearity of the unstratified shearing box system, keeping only those interactions that involve the $k_x = k_y = 0$ modes (the mean fields), thus eliminating a turbulent cascade. Our primary result is that despite this huge simplification – the only nonlinearity is due to the mean field dynamo – the quasi-linear system displays similar trends to fully developed MRI turbulence. In particular, a decrease in Re at fixed Rm (*i.e.*, an increase in Pm), causes an increase in angular momentum transport. This unintuitive scaling is the same as that observed self-sustaining nonlinear

turbulence, illustrating that such effects are at least partially due to the large scale dynamo in the system, and facilitating possible future semi-analytic studies of the very high/low Pm regimes. In addition, direct statistical simulation (the CE2 method) [18, 19] provides very clear information on the bifurcations between turbulent states of the system. We see two important bifurcations as Rm is increased: the first is the transition from stable homogenous turbulence to a stable inhomogenous equilibrium with strong mean-fields (the dynamo instability), the second a loss of stability of the inhomogenous equilibrium and transition to a near-periodic time-dependent state. Given the strong dependence of both the saturated states and the second bifurcation on Pm, as well as the marked similarity to quasi-linear studies of plane Couette flow [20], it seems likely that further study of this dynamo instability will yield important insights into the fundamental nature of the MRI system.

We extend thanks to Jim Stone, Jiming Shi and John Krommes for enlightening discussion. This work was supported by Max Planck/Princeton Center for Plasma Physics and U.S. DOE (DE-AC02-09CH11466).

[1] S. A. Balbus and J. F. Hawley, Rev. Mod. Phys. **70**, 1 (1998).

[2] S. Fromang and J. Papaloizou, Astron. Astrophys. **476**, 1113 (2007).

[3] G. Bodo, A. Mignone, F. Cattaneo, P. Rossi, and A. Ferrari, Astron. Astrophys. **487**, 1 (2008).

[4] J. Shi, J. H. Krolik, and S. Hirose, Astrophys. J. **708**, 1716 (2010).

[5] S. W. Davis, J. M. Stone, and M. E. Pessah, Astrophys. J. **713**, 52 (2010).

[6] P. Y. Longaretti and G. Lesur, Astron. Astrophys. **516**, 51 (2010).

[7] J. B. Simon, K. Beckwith, and P. J. Armitage, Mon. Not. R. Astron. Soc. **422**, 2685 (2012).

[8] G. Bodo, F. Cattaneo, A. Mignone, and P. Rossi, Astrophys. J. **787**, L13 (2014).

[9] S. Fromang, J. Papaloizou, G. Lesur, and T. Heinemann, Astron. Astrophys. **476**, 1123 (2007).

[10] S. Fromang, Astron. Astrophys. **514**, L5 (2010).

[11] J. B. Simon, J. F. Hawley, and K. Beckwith, Astrophys. J. **730**, 94 (2011).

[12] J. S. Oishi and M.-M. Mac Low, Astrophys. J. **740**, 18 (2011).

[13] M. Flock, T. Henning, and H. Klahr, Astrophys. J. **761**, 95 (2012).

[14] P. J. Käpylä and M. J. Korpi, Mon. Not. R. Astron. Soc. **413**, 901 (2011).

[15] G. Lesur and G. I. Ogilvie, Astron. Astrophys. **488**, 451 (2008).

[16] O. Gressel, Mon. Not. R. Astron. Soc. **405**, 41 (2010).

[17] F. Ebrahimi and A. Bhattacharjee, Phys. Rev. Lett. **112**, 125003 (2014).

[18] B. F. Farrell and P. J. Ioannou, J. Atmos. Sci. **60**, 2101 (2003).

[19] J. B. Marston, E. Conover, and T. Schneider, J. Atmos. Sci. **65**, 1955 (2008).

[20] B. F. Farrell and P. J. Ioannou, J. Fluid Mech. **708**, 149 (2012).

[21] S. M. Tobias, K. Dagon, and J. B. Marston, Astrophys. J. **727**, 127 (2011).

[22] K. Srinivasan and W. R. Young, J. Atmos. Sci. **69**, 1633 (2012).

[23] J. B. Parker and J. A. Krommes, Phys. Plasmas **20**, 100703 (2013).

[24] J. Squire and A. Bhattacharjee, Phys. Rev. Lett. **113**, 025006 (2014).

[25] F. Rincon, G. I. Ogilvie, and M. R. E. Proctor, Phys. Rev. Lett. **98**, 254502 (2007).

[26] A. Riols, F. Rincon, C. Cossu, G. Lesur, P. Y. Longaretti, G. I. Ogilvie, and J. Herault, J. Fluid Mech. **731**, 1 (2013).

[27] Eq. (3), the basis for the CE2 system, can also be derived as a truncation of the cumulant expansion at second order, see Ref. [21].

[28] Y. Lithwick, Astrophys. J. **670**, 789 (2007).

[29] This may not be the case at the highest Rm studied, since $\bar{\boldsymbol{U}}$ grows slowly but does not ever get small enough relative to $\bar{\boldsymbol{B}}$ to say for sure whether the eigenmode satisfies $\bar{\boldsymbol{U}} = 0$ or just $\bar{\boldsymbol{U}} \ll \bar{\boldsymbol{B}}$. In either case, it is far too small to be of dynamical importance in the linear growth phase.

[30] G. Lesur and G. I. Ogilvie, Mon. Not. R. Astron. Soc. **391**, 1437 (2008).

[31] A. Brandenburg, Astrophys. J. **697**, 1206 (2009).

[32] N. C. Constantinou, A. Lozano-Durán, M.-A. Nikolaidis, B. F. Farrell, P. J. Ioannou, and J. Jimenez, J. Phys.: Conference Series **506**, 012004 (2014).

Princeton Plasma Physics Laboratory
Office of Reports and Publications

Managed by
Princeton University

under contract with the
U.S. Department of Energy
(DE-AC02-09CH11466)

P.O. Box 451, Princeton, NJ 08543
Phone: 609-243-2245
Fax: 609-243-2751

E-mail: publications@pppl.gov
Website: http://www.pppl.gov